

## EFFECT OF SUBELEMENT SPACING IN RRP Nb<sub>3</sub>SN STRANDS

E. Barzi<sup>1</sup>, D. Turrioni<sup>1</sup>, M. Alsharo'a<sup>2</sup>, M. Field<sup>3</sup>, S. Hong<sup>3</sup>, J. Parrell<sup>3</sup>,  
R. Yamada<sup>1</sup>, Y. Zhang<sup>3</sup>, and A. V. Zlobin<sup>1</sup>

<sup>1</sup> Fermi National Accelerator Laboratory  
Batavia, IL, 60510, USA

<sup>2</sup> Muons, Inc.  
Batavia, IL, 60510, USA

<sup>3</sup> Oxford Instruments Superconducting Technology  
Carteret, NJ, 07008, USA

### ABSTRACT

The Restacked Rod Process (RRP) is the Nb<sub>3</sub>Sn strand technology presently producing the largest critical current densities at 4.2 K and 12 T. However, when subject to plastic deformation, RRP subelements (SE) were found to merge into each other, creating larger filaments with a somewhat continuous barrier. In this case, the strand sees a larger effective filament size,  $d_{\text{eff}}$ , and its instability can dramatically increase locally leading to cable quench. To reduce and possibly eliminate this effect, Oxford Instruments Superconducting Technology (OST) developed for FNAL a modified RRP strand design with larger Cu spacing between SE's arranged in a 60/61 array. Strand samples of this design with sizes from 0.7 to 1 mm were first evaluated for transport current properties. A comparison study was then performed between the regular 54/61 and the modified 60/61 design using 0.7 mm round and deformed strands. Finite element modeling of the deformed strands was also performed with ANSYS.

**KEYWORDS:** Nb<sub>3</sub>Sn, Restacked Rod Process, critical current density, magnetic instability.

**PACS:** 74.70.Ad.

**TABLE 1.** Strand Description

Strand ID	RRP1	RRP2
No. of subelements	60/61	54/61
Strand diameter, mm	0.7	0.7
Geometric filament size, $\mu\text{m}$	57-71	59-74
Twist pitch, mm	12	13.5
Cu fr., %	46	46.5

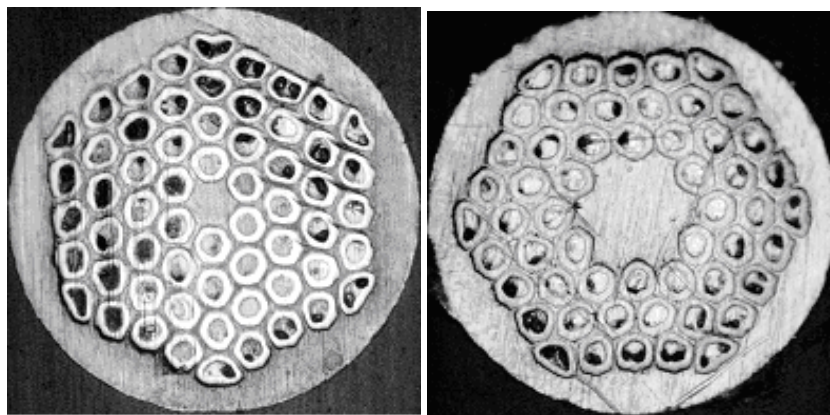
## INTRODUCTION

Using microscopic analysis, it has already been shown that the modified RRP 60/61 design produced by OST with increased thickness between subelements is effective in reducing subelement merging under plastic deformation. The larger Cu thickness provides a barrier to merging not as much during the deformation process as during reaction [1]. This paper, rather, is concerned with the transport current properties of the modified 60/61 design strand. To first evaluate the improved 60/61 design using strands of various sizes, they were all initially given the same relative deformation, i.e.  $\sim 30\%$ . Rolling was the method that was chosen as it produces a homogenous deformation along the length of the strand. A subsequent comparison study between the regular 54/61 design and the spaced 60/61 design was performed on 0.7 mm strands, which were rolled down to a number of thickness values to cover a large range of deformations. This study compares the effect of increasing deformation on  $I_c$ ,  $I_s$  and RRR between the two designs. An ANSYS finite element model validated with experimental data was then implemented to simulate plastic deformation of both strand designs.

## EXPERIMENTAL SETUP

### Strand Description

Table 1 shows parameters of the 60/61 subelement strand with increased Cu spacing (RRP1), and of a strand (RRP2) representing the latest generation of the original 54/61 subelement design [2]. Pictures of the cross sections are in Figure 1. With the appropriate heat treatment, the RRP1 strand produced a  $J_c(4.2\text{K}, 12\text{T})$  of  $3269 \text{ A/mm}^2$ , as measured by OST.

**FIGURE 1.** RRP1 strand with 60/61 spaced subelements (left), and RRP2 strand with 54/61 regular subelements (right).

## Sample Preparation and Measurement Procedure

The strand samples were wound and heat treated in Argon atmosphere on grooved cylindrical barrels made of Ti-alloy. All the strands used in this study were given the same heat treatment schedule of 25°C/h up to 210°C, 50 h; 50°C/h up to 400°C, 50 h; 75°C/h up to 640°C, 60 h. After reaction, the samples were tested on the same barrel. The  $I_c$  was determined from the voltage-current (V-I) curve using the  $10^{-14}$   $\Omega\cdot\text{m}$  resistivity criterion. The stability current,  $I_s$ , is obtained through V-H tests as the minimum quench current in the presence of a magnetic field variation. To test  $I_c$  and  $I_s$ , two orientations were used for the rolled strand with respect to the external magnetic field. In the so-called short edge configuration, the longest size of the strand is perpendicular to the field, and in the long edge configuration, it is the shortest size of the strand that is perpendicular to the field. In the former case, which is less mechanically stable, STYCAST was used for the sample, whereas in the latter case no bonding agent was used. Unless otherwise specified, all test results were obtained at 4.2 K.

## RESULTS AND DISCUSSION

### First Evaluation Study

This study was performed on strand samples of three different sizes, 1 mm, 0.8 mm and 0.7 mm, from billet RRP1. These were all given the same relative deformation, i.e. ~30%, to be then compared with their round counterparts. Numeric results are shown in Table 2. The range of values in the round strand columns represent the results obtained when testing without and with a bonding agent. The  $J_c(12\text{ T})$  of round strands tested with STYCAST is typically 5% larger than those tested without. However, this effect is larger for the rolled strands. The difference in  $J_s$  when testing with the two different magnetic field orientations is between 20 and 40%. Whereas the  $J_c(12\text{ T})$  is very similar for all round strands, Figure 2 (left) shows a clear dependence of  $J_s$  with subelement size. Figure 2 (right) shows an interesting additional effect, which is that smaller subelements are less sensitive to  $I_c$  degradation.

### $I_c$ in the Comparison Study

In the following, because of the very similar Cu% of the strands under comparison, absolute as opposed to normalized properties are shown. In addition, these are given as a function of actual deformed strand size, as measured by microscopy, as opposed for instance to relative strand deformation. Figures 3 and 4 show the  $I_c(12\text{ T})$  comparison between the regular

**TABLE 2.** Results of First Evaluation Study

Def. state	Round	Rolled		Round	Rolled		Round	Rolled	
Size	1.0 mm	to 0.7 mm		0.8 mm	to 0.56 mm		0.7 mm	to 0.5 mm	
Test config.		Long edge	Short edge (w/sty)		Long edge	Short edge (w/sty)		Long edge	Short edge (w/sty)
$I_c(12\text{T}), \text{A}$	1114-1159	857	925	713-732	538	639	547-571	487	518
$J_c(12\text{T}), \text{A}/\text{mm}^2$	2627-2733	2021	2181	2627-2697	1982	1507	2632-2748	2343	1221
$I_s, \text{A}$	1350-1400	1400	1150	1200-1350	900	1050	1200-1300	750	850
$J_s(12\text{T}), \text{A}/\text{mm}^2$	3183-3301	3301	2712	4421-4974	3316	2476	5744-6256	3609	2004
RRR	180-182	124	115	145-185	83	87	194-212	61	89

54/61 design and the spaced 60/61 design in the short edge (with STYCAST) and long edge (without bonding agent) configuration respectively. Typical  $I_c$  measurement uncertainties are within  $\pm 1\%$  at 4.2 K and 12 T. It can be seen that the 60/61 round strand has a slightly better  $I_c$  performance. However, the  $I_c$  (12 T) degrades similarly under increasing deformation for the two strands, which is consistent with the two designs having similar subelement sizes.

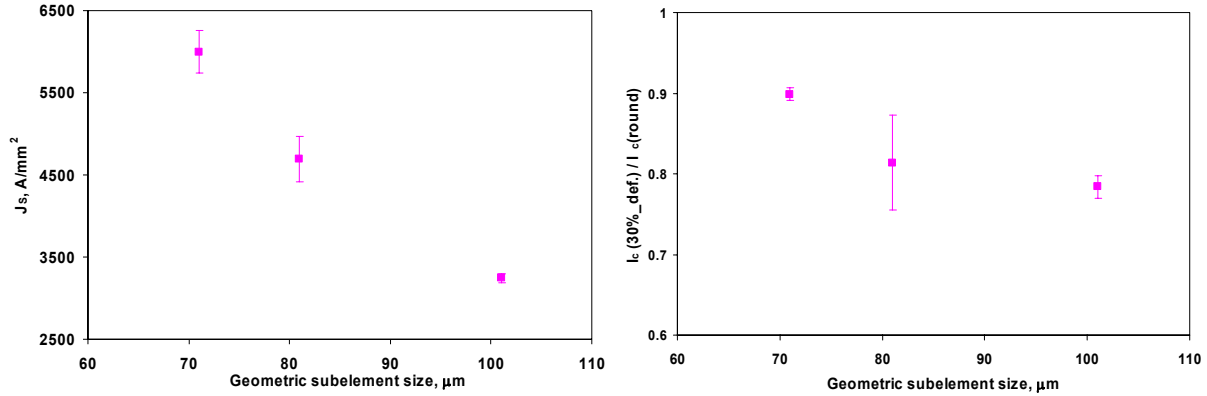


**FIGURE 2.**  $J_s$  of the RRP1 round strand as a function of geometric subelement size (left),  $I_c$  degradation at 12 T of RRP1 strands after a 30% deformation as a function of geometric subelement size of the round strand (right).

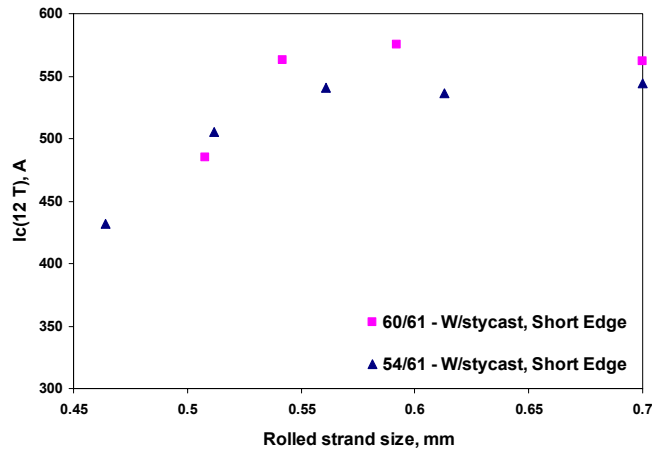


**FIGURE 3.**  $I_c(12 T)$  of the round and rolled strands tested with STYCAST in the short edge configuration as a function of actual deformed strand size.

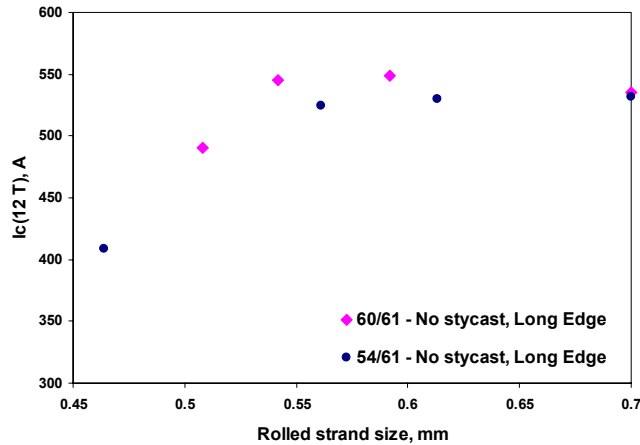


**FIGURE 4.**  $I_c(12 T)$  of the round and rolled strands tested with no bonding agent in the long edge configuration as a function of actual deformed strand size.

### I<sub>s</sub> in the Comparison Study

Figures 5 and 6 show the I<sub>s</sub> comparison between the regular 54/61 design and the spaced 60/61 design in the short edge (with STYCAST) and long edge (without bonding agent) configuration respectively. In the former case, some of the samples were tested in a test station with a 1020 A power supply limit. Typical I<sub>s</sub> reproducibilities when testing similar samples is within 20%. It can be seen that the 60/61 strand has a systematically better I<sub>s</sub> performance over most of the deformation range, which is consistent with its reduced sensitivity to merging [1].

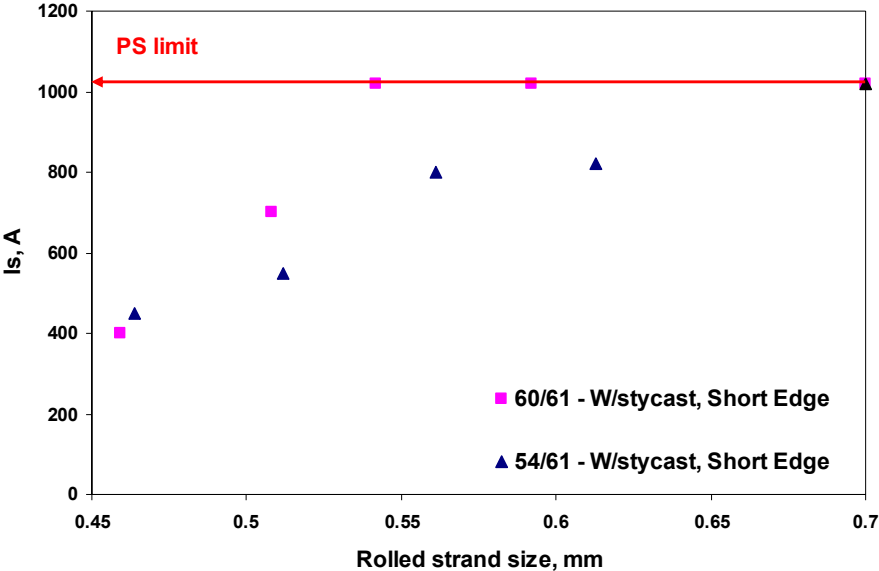


FIGURE 5. I<sub>s</sub> of the round and rolled strands tested with STYCAST in the short edge configuration as a function of actual deformed strand size.

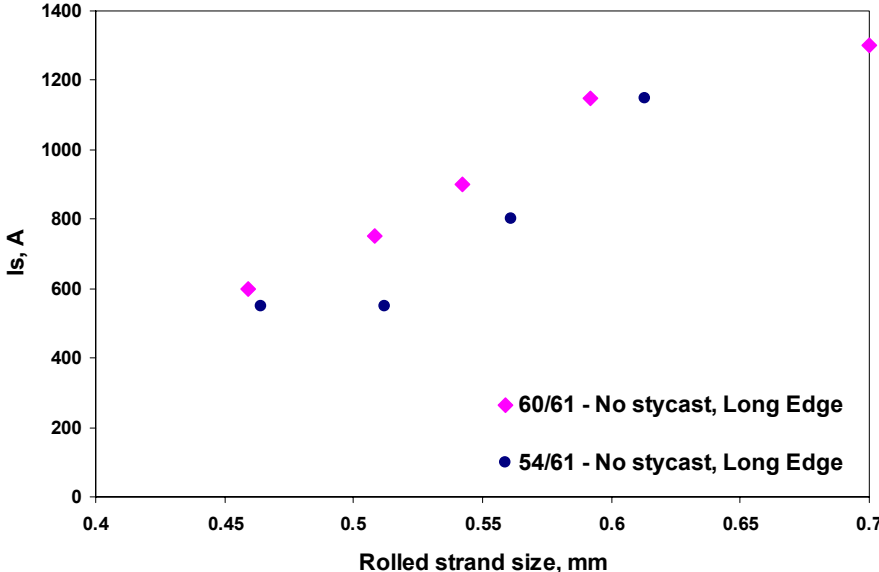
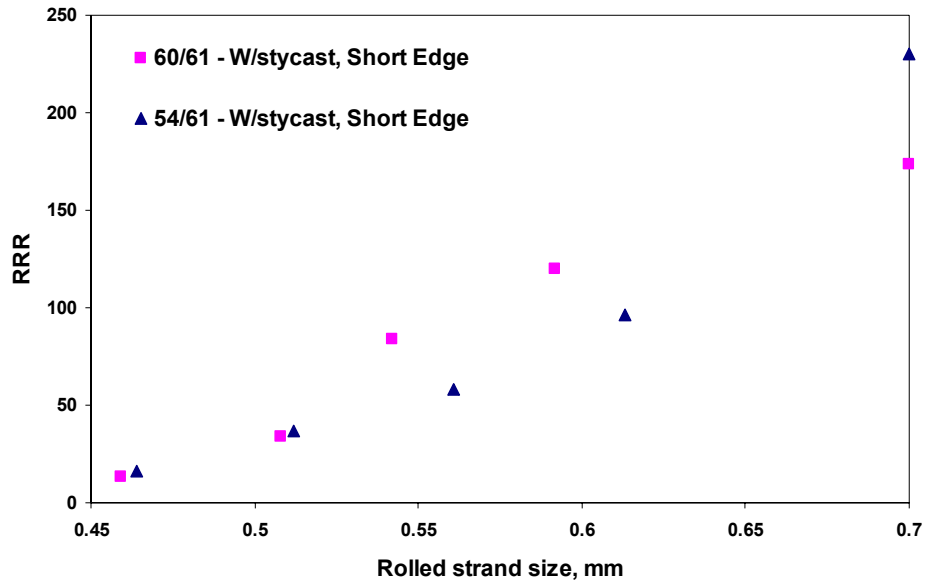


FIGURE 6. I<sub>s</sub> of the round and rolled strands tested with no bonding agent in the long edge configuration as a function of actual deformed strand size.

## RRR in the Comparison Study

Figures 7 and 8 show the RRR comparison between the regular 54/61 design and the spaced 60/61 design in the short edge (with STYCAST) and long edge (without bonding agent) configuration respectively. In this case the better capability of the 60/61 strand to withstand deformation is even more obvious. Despite a lower original RRR value in the round strand, in the rolled strands it shows consistently larger RRR values up to a relative deformation of 30%.



**FIGURE 7.** RRR of the round and rolled strands with STYCAST in the short edge configuration as a function of actual deformed strand size.

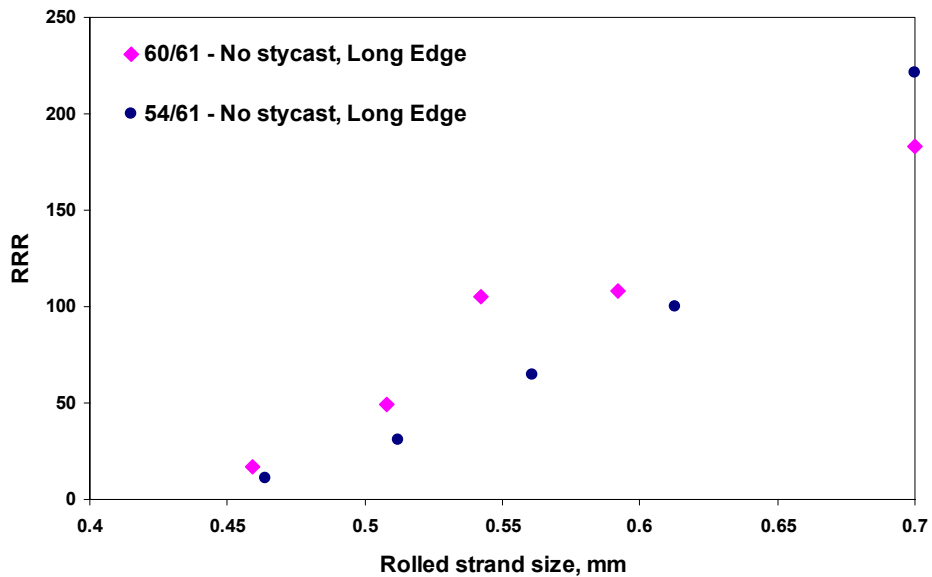


**FIGURE 8.** RRR of the round and rolled strands tested with no bonding agent in the long edge configuration as a function of actual deformed strand size.

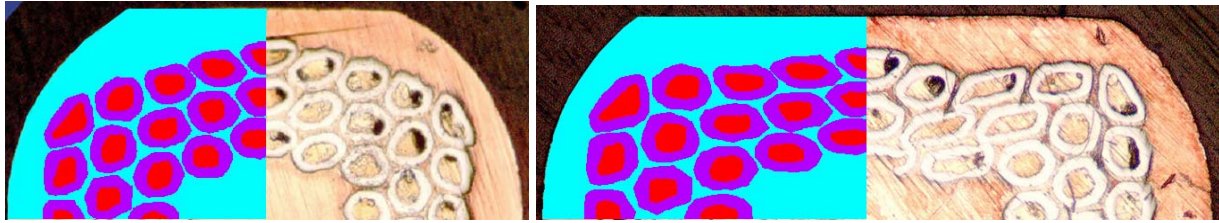


FIGURE 9. ANSYS model of 54/61 strand deformed to 0.6 mm (left) and to 0.5 mm (right).

## Finite Element Modeling

To model strand deformation with ANSYS [3], parallel contact surfaces were used to apply a load to a round composite made of Sn and Nb subelements embedded in a Cu matrix [4]. The SE shape was modeled as close as possible to the real one using microscopy pictures of the strand cross sections. To model plastic behavior, material properties over both the elastic and plastic strain ranges were used [5]. The model was validated through comparisons of the predicted deformed strand shape with a number of microscopy pictures of strand cross sections at each deformation stage (see for instance Figure 9). The present simulation procedure does not model SE fracture or merging. However an excellent correlation was found in final deformed strand shapes up to relative deformations of  $\sim 30\%$ .

Comparison of the simulation results between the regular 54/61 strand and the spaced 60/61 strand design shows that in the former case SE's start touching already at a relative deformation of 15%, whereas in the latter, SE's do not touch each other at least up to a relative deformation of 35%. This would be consistent with the lower merging as seen in the 60/61 design [1]. The strain parallel to the applied load,  $\epsilon_y$ , in the Nb tubes is typically larger in the 54/61 design, as shown in Figure 10 (left). However, the shear strain  $\epsilon_{xy}$  is very similar in both designs, which again would be consistent with their similar level of SE breakage [1].

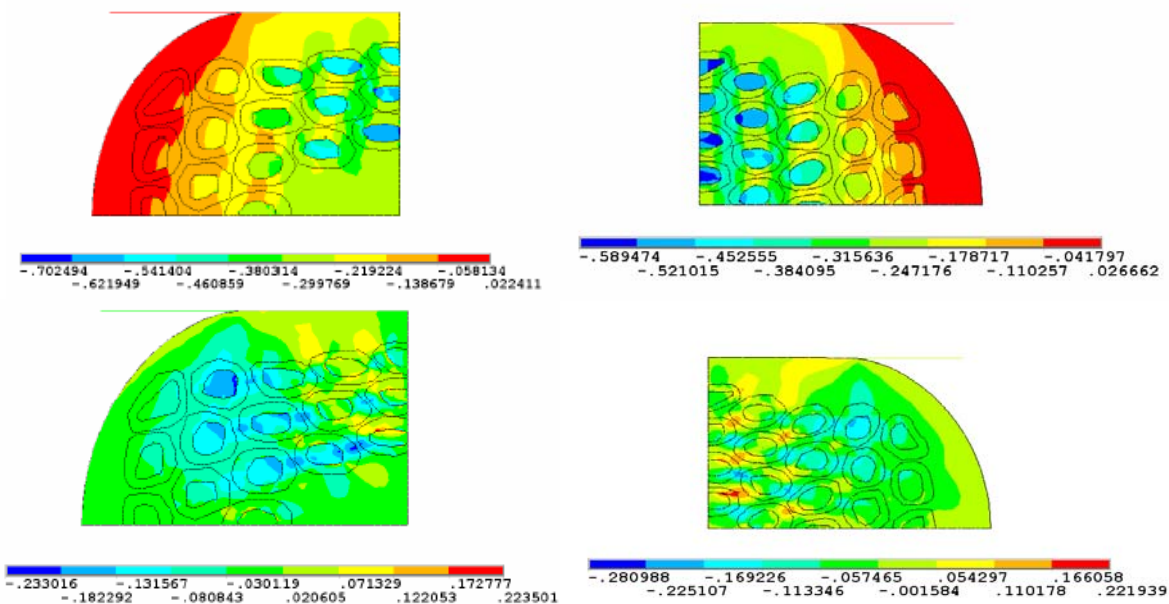


FIGURE 10. Vertical strain  $\epsilon_y$  (top left) and shear strain  $\epsilon_{xy}$  (bottom left) for the 0.7 mm 54/61 strand deformed to 0.5 mm, and vertical strain  $\epsilon_y$  (top right) and shear strain  $\epsilon_{xy}$  (bottom right) for the 0.7 mm 60/61 strand deformed to 0.5 mm as obtained with an ANSYS model.

## CONCLUSIONS

Using microscopic analysis, the modified 60/61 design produced by OST with increased thickness between subelements and slightly smaller SE size was proven to be effective in reducing merging [1]. A first electrical evaluation study performed on strand samples of different sizes showed a clear dependence of  $J_s$  with SE size as expected. When given the same 30% relative deformation, it was also found that smaller SE's are less sensitive to  $I_c$  degradation.

For a fair comparison between the regular 54/61 design and the spaced 60/61 design, a billet representing the latest generation of the original 54/61 design was chosen with very similar Cu%. Strands of 0.7 mm size were used to be rolled down to a number of thickness values to cover a large range of deformations. This study, which compared the effect of increasing deformation on  $I_c$ ,  $I_s$  and RRR between the two designs, showed the following results. The  $I_c(12\text{ T})$  degraded similarly under increasing deformation for the two strands. This is consistent with the two designs having similar SE sizes. The 60/61 strand had a systematically better  $I_s$  performance over most of the deformation range. This is consistent with its reduced sensitivity to merging and possibly with its smaller  $d_{\text{eff}}$ . Despite a lower original RRR value in the round strand, in the rolled strands the 60/61 showed consistently larger RRR values over most of the deformation range. In this case the better capability of the 60/61 strand to withstand deformation is even more obvious.

ANSYS results of plastic modeling of the two designs were consistent with the lower SE merging and similar SE breakage observed through microscopic analysis in the 60/61 design [1]. These coherent results from microscopy, transport properties, and modeling clearly show that increasing Cu spacing between SE's is beneficial to the RRP technology, in that it allows making a better use of its  $J_c$  potential by reducing the risk of merging, and therefore of instabilities. To keep improving RRP properties, the next R&D step with OST has been that of implementing the same spacing concept to billets with a larger number of restacks.

## ACKNOWLEDGMENTS

We thank the technical staff of the Superconductor R&D group at FNAL, Marianne Bossert, Al Rusy and Tom VanRaes, whose skills and commitment were essential for this work.

## REFERENCES

1. D. Turrioni et al., "Study of Effects of Deformation in  $Nb_3Sn$  Multifilamentary Strands", Applied Superconductivity Conference, Aug. 27-Sep. 1, 2006, Seattle, WA. Paper accepted for publication in IEEE Trans. Appl. Superconductivity.
2. E. Barzi et al., "RRP  $Nb_3Sn$  Strand Studies for LARP", Applied Superconductivity Conference, Aug. 27-Sep. 1, 2006, Seattle, WA. Paper accepted for publication in IEEE Trans. Appl. Superconductivity.
3. ANSYS, Inc. [www.ansys.com](http://www.ansys.com).
4. S. Farinon et al., "Finite element model to study the deformations of  $Nb_3Sn$  wires for the Next European Dipole (NED)", Applied Superconductivity Conference, Aug. 27-Sep. 1, 2006, Seattle, WA. Paper accepted for publication in IEEE Trans. Appl. Superconductivity.
5. The Materials Information Society, "Atlas of Stress-Strain Curves", ASM International, Second Edition.